Finite element beam propagation method for analysis of plasmonic waveguide

Jianjun Chen (陈建军)[1,2], Zhaofeng Li (李兆峰)[2], Zhongchao Fan (樊中朝)[1], and Fuhua Yang (杨富华)[1,2]

[1]*Research Center of Semiconductor Integration, Institute of Semiconductors, Chinese Academy of Sciences, Beijing 100083*

[2]*State Key Laboratory for Superlattices and Microstructures, Institute of Semiconductors, Chinese Academy of Sciences, Beijing 100083*

Received December 11, 2007

The basic idea of the finite element beam propagation method (FE-BPM) is described. It is applied to calculate the fundamental mode of a channel plasmonic polariton (CPP) waveguide to confirm its validity. Both the field distribution and the effective index of the fundamental mode are given by the method. The convergence speed shows the advantage and stability of this method. Then a plasmonic waveguide with a dielectric strip deposited on a metal substrate is investigated, and the group velocity is negative for the fundamental mode of this kind of waveguide. The numerical result shows that the power flow direction is reverse to that of phase velocity.

OCIS codes: 000.3860, 130.0130, 240.0240.
doi: *10.3788/COL20080608.0572.*

Surface plasmonic polariton (SPP) is a kind of light wave that occurs at a metal/dielectric interface. The advantage of SPP is to shrink the size of optical devices greatly, which makes a big opportunity for photonic integration[1−6]. However, the propagation length of plasmon waveguide is limited. Some methods have been offered to solve this problem[7−9]. Here, we took a fast, convenient and precise numerical method, the finite element beam propagation method (FE-BPM), to calculate the modes of the plasmonic waveguide. It has already been developed and applied to photonic crystal fibers[10,11]. Finite element method can deal with fine and complex structure, which has advantage over the finite difference method. Because of the negative permittivity of metals, the light flow in SPP waveguide is not like that in conventional waveguides.

From Maxwell equations, the following vectorial wave equation is derived:

$$\nabla \times (p\nabla \times \mathbf{\Phi}) - k_0^2 q\mathbf{\Phi} = 0, \tag{1}$$

where $\mathbf{\Phi}$ denotes either electric field $\mathbf{E}$ or magnetic field $\mathbf{H}$, p and q are given by

$$\begin{cases} p = 1, \quad q = n^2 \text{ for } \mathbf{\Phi} = \mathbf{E} \\ p = 1/n^2, \quad q = 1 \text{ for } \mathbf{\Phi} = \mathbf{H} \end{cases}. \tag{2}$$

Using an appropriate reference refractive index n_0 and slowly varying envelop approximation which are widely used in beam propagation method (BPM)[10], the solution form was written as

$$\begin{aligned} \mathbf{\Phi}(x,y,z) = {} & \boldsymbol{\phi}_t(x,y,z)\exp(-jk_0n_0z) \\ & + \boldsymbol{\phi}_z(x,y,z)\exp(-jk_0n_0z), \end{aligned} \tag{3}$$

where $\boldsymbol{\phi}_t(x,y,z) = \phi_x(x,y,z)\hat{x} + \phi_y(x,y,z)\hat{y}$ is the field component in the x-y plane.

Expanding the transverse fields ϕ_x and ϕ_y, and the axial field ϕ_z in each element as

$$\boldsymbol{\phi} = \begin{bmatrix} \phi_x \\ \phi_y \\ \phi_z \end{bmatrix} = \begin{bmatrix} \{\mathbf{U}\}^{\mathrm{T}}\{\phi_t\}_e \\ \{\mathbf{V}\}^{\mathrm{T}}\{\phi_t\}_e \\ j\{\mathbf{N}\}^{\mathrm{T}}\{\phi_z\}_e \end{bmatrix}, \tag{4}$$

where $\{\mathbf{U}\}$, $\{\mathbf{V}\}$, and $\{\mathbf{N}\}$ are shape function vectors[10−14], which are determined by the coordinates of vertex of each triangular element. The element type used here is the hybrid edge-nodal element[14].

Substituting Eq. (4) into Eq. (1), neglecting the second order part of the z-component, and applying the finite element technique to the transverse plane, we got the following matrix equation[11]:

$$[\mathbf{A}]_i\{\phi\}_{i+1} = [\mathbf{B}]_i\{\phi\}_i, \tag{5}$$

where $[\mathbf{A}]_i$ and $[\mathbf{B}]_i$ are functions about $\{\mathbf{U}\}$, $\{\mathbf{V}\}$, and $\{\mathbf{N}\}$ at step i[11]. The BPM formulation comes into being at last. The imaginary distance propagation scheme of BPM method[10,11,15] was used in our work. The fundamental mode was firstly calculated. For stability, the longitudinal-field component was transformed[16].

The imaginary distance method assumed the propagation length z as an imaginary value. For all modes existing in the waveguide, the fundamental mode has the largest real part of wave vector. When propagating the imaginary distance z, it has the largest magnification coefficient of $\exp(\mathrm{Re}(k)\,\mathrm{Im}(z))$. With several times of iterations, the fundamental mode dominates the field and all the other modes are suppressed.

To get higher order modes, we just need to normalize and remove the modes having been calculated, and then repeat the FE-BPM[10]. Perfectly matched layer (PML) is applied here as boundary condition for convenience and versatility[13,17,18].

We considered a channel plasmonic polariton (CPP) waveguide that has been solved by the finite difference method in Ref. [19]. An air slot in a thin silver film ($\varepsilon_{\mathrm{Ag}} = -122 + 9i$ at the free space wavelength $\lambda =$

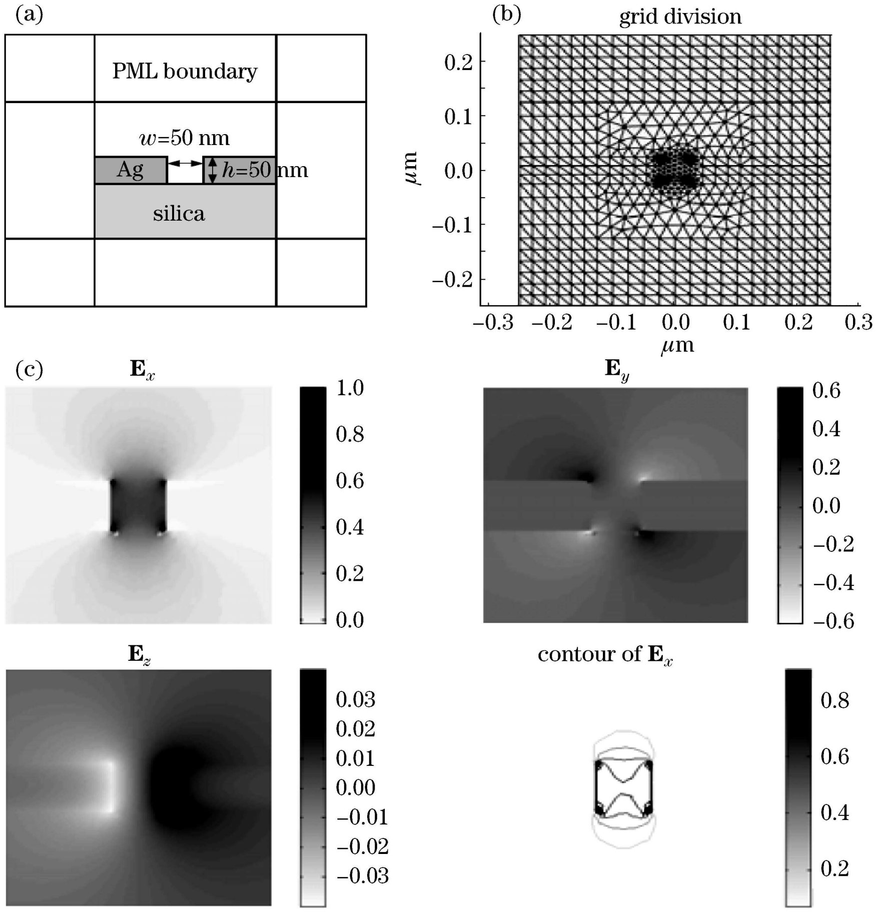

Fig. 1. (a) Schematic of the cross section of a CPP waveguide. It is invariant along the longitudinal direction; (b) grid division profile with triangular elements; (c) electric field distributions for the fundamental mode of the CPP waveguide.

1.55 μm) was deposited on a silica substrate ($n_s = 1.44$), as shown in Fig. 1(a). Figure 1(b) shows the element division profile of this structure.

Figure 1(c) gives the electric field distribution for the fundamental mode at 1.55 μm. The effective index of this mode is $1.5414 - 0.0126i$, the real component of which is larger than both the refractive index of air and the refractive index of silica. The imaginary part of the effective index determines the propagation length of the plasmonic waveguide. It is the ohmic heating loss in the metal that limits the propagation length of plasmonic waves to only about 20 μm. Such a length is small but enough for a nanometer sized waveguide.

Figure 2 shows the convergence of the imaginary distance BPM. After seven steps of iteration, the effective index becomes a constant value. The initial field for the BPM is a random field that may include all modes. As the iteration steps increase, the fundamental mode dominates the field. So the imaginary part decreases from a large value to nearly zero.

The schematic representation of the second case is shown in Fig. 3(a). It is discussed by Karalis *et al.*[20]. By changing the thickness of the dielectric strip, the velocity of plasmon can be controlled. The waveguide exhibits negative group velocity at certain frequency range. We studied the mode when the negative group velocity occurs. The result shows that the effective index of the

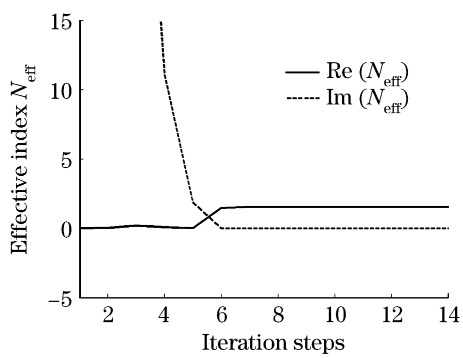

Fig. 2. Convergence of the mode effective index with the iteration steps.

fundamental mode is $N_{\text{eff}} = 5.4700 + 0.5655i$ at 500 nm. The positive imaginary part means the power magnifies along the wave propagation direction. It seems contrary to the conversation of energy law, but it can be explained by the negative group velocity.

The magnetic field distribution is shown in Fig. 3(b). It is strongly confined around the dielectric strip. Figure 3(c) shows the time averaged Poynting vector distribution along z direction. The sign of Poynting vector at the dielectric side is positive ($S_z^+(x,y)$) while at the metal side negative ($-S_z^-(x,y)$). We integrated Poynting vector over the computational window, and got a result

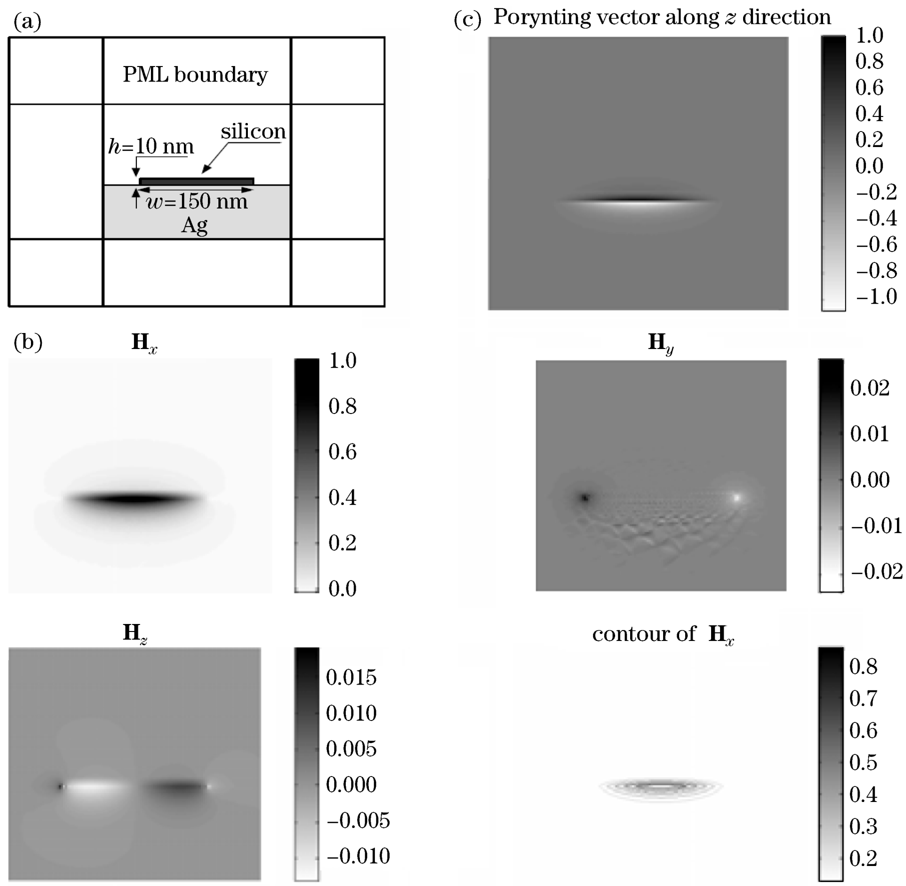

Fig. 3. (a) Schematic of the cross section of a plasmonic waveguide, a thin silicon dielectric strip is deposited on the silver substrate; (b) magnetic field distributions for the fundamental mode in the plasmonic waveguide; (c) field distribution of the time averaged Poynting vector along the longitudinal direction.

$(S_z^+ - S_z^-)/(S_z^+ + S_z^-) = -0.183$. It means that the power flow is just like a vortex, and the back flow in the metal side is the dominant one. Such an energy vortex forms the negative group velocity of this kind of plasmonic waveguide.

We have applied the FE-BPM to calculate the mode pattern of plasmonic waveguides. Our works show that it is an appropriate numerical method for plasmonic waveguide because it converges fast, gives an accurate result, and deals with complex structures easily. A CPP waveguide and a plasmonic waveguide with negative group velocity are investigated. The latter one may also be a good proposal to make negative refractive meta-materials in optical wavelength ranges because of its simple structure.

This work was supported by the National Natural Science Foundation of China under Grant No. 60707009. J. Chen's e-mail address is jjchen@semi.ac.cn.

References

1. E. Ozbay, Science **311,** 189 (2006).
2. H. Zhao, X. Huang, and H. Su, Acta Opt. Sin. (in Chinese) **27,** 1649 (2007).
3. H. Raether, *Surface Plasmons* (Springer, Berlin, 1988).
4. S. I. Bozhevolnyi, V. S. Volkov, E. Devaux, J.-Y. Laluet, and T. W. Ebbesen, Nature **440,** 508 (2006).
5. S. I. Bozhevolnyi, V. S. Volkov, E. Devaux, and T. W. Ebbesen, Phys. Rev. Lett. **95,** 046802 (2005).
6. D. K. Gramotnev and D. F. P. Pile, Appl. Phys. Lett. **85,** 6323 (2004).
7. M. P. Nezhad, K. Tetz, and Y. Fainman, Opt. Express **12,** 4072 (2004).
8. M. Hochberg, T. Baehr-Jones, C. Walker, and A. Scherer, Opt. Express **12,** 5481 (2004).
9. D. J. Bergman and M. I. Stockman, Phys. Rev. Lett. **90,** 027402 (2003).
10. S. S. A. Obayya, B. M. A. Rahman, K. T. V. Grattan, and H. A. El-Mikati, J. Lightwave Technol. **20,** 1054 (2002).
11. K. Saitoh and M. Koshiba, IEEE J. Quantum Electron. **38,** 927 (2002).
12. M. Koshiba, *Optical Waveguide Theory by the Finite Element Method* (KTK, Holland, 1992).
13. J. M. Jin, *The Finite Element Method in Electromagnetics* (Wiley, New York, 1993).
14. M. Koshiba and Y. Tsuji, J. Lightwave Technol. **18,** 737 (2000).
15. C. L. Xu, W. P. Huang, and S. K. Chaudhuri, J. Lightwave Technol. **11,** 1209 (1993).
16. D. Schulz, C. Glingener, M. Bludszuweit, and E. Voges, J. Lightwave Technol. **16,** 1336 (1998).
17. W. P. Huang, C. L. Xu, W. Lui, and K. Yokoyama, IEEE Photon. Technol. Lett. **8,** 649 (1996).
18. M. Koshiba, Y. Tsuji, and M. Hikari, IEEE Trans. Magn. **35,** 1482 (1999).
19. G. Veronis and S. Fan, Proc. SPIE **6123,** 612308 (2006).
20. A. Karalis, E. Lidorikis, M. Ibanescu, J. D. Joannopoulos, and M. Soljačić, Phys. Rev. Lett **95,** 063901 (2005).